Copy number of transfectants was determined by Southern blotting using a probe in *Xist* exon 6 (probe B in Fig. 1) which differentiates between exogenous *Xist* sequence and the transgene by a unique *Eco*RI restriction site in the cosmid. PhosphorImager analysis indicated that cosmid copy numbers were 6, 2, and 8 for transfectants zHβ2, zHβ5, and zHβ10, respectively. Further analysis using probes for 5′ *Xist* exon 1 or β-Gal (probes A, C in Fig. 1) indicated that the cosmid integrants were probably intact. FISH analysis of zHβ2 and zHβ10 confirmed that integrants were at single distinct autosomal sites in the genome.

LacZ-positive, G418-resistant ES cell transfectants were differentiated by EB formation as follows: semiconfluent ES cell populations were lightly trypsinized and cell clusters were cultured in suspension on bacterial dishes in DMEM medium supplemented with 10% FCS, without LIF feeder cells or G418, for 4–5 days. To analyse LacZ-staining activity and sensitivity to G418 upon differentiation, individual EBs were aspirated and plated into gelatinized 96-well dishes and allowed to adhere. 1–3 days later, half of the adhered blasts were transferred to medium containing G418, and 5–10 days later stained for LacZ activity using X-Gal[22]. For temporal analysis of LacZ staining during differentiation, EB samples were collected from suspension cultures and stained with X-Gal at 24-h intervals.

RNA analysis. ES cells were prepared for RNA isolation by multiple passages onto gelatinized dishes without feeder cells to prevent contamination by feeder-derived RNA. EBs were cultured in suspension for 8–10 days and collected for RNA preparation when the majority of EBs had become cystic. RNA was isolated using RNAzol B (Biogenesis Ltd) according to the manufacturer's instructions. 10 μg of each RNA sample was electrophoresed on a 1% agarose gel containing formaldehyde and blotted onto Hybond N. The *Xist* probe was a 9.5-kb PCR fragment derived from exon 1 of the *Xist* gene. β-Gal RNA was detected with probe C (Fig. 1). Cosmid *Xist* (C57BL/10-strain-derived) and CCE ES cell *Xist* (129-strain-derived) were distinguished by a single base difference[17]. As the polymorphism is within a poly(A) tract, it is not amenable to direct analysis. cDNA flanking the polymorphism was amplified by RT-PCR (primers were 5′-ACGCGTCGACGTGTGTATGGTGG ACTTACC-3′ and 5′-CCATCGATATCAGCAGCAACAGTACACG-3′) from RNA prepared from the transfectants and subcloned into pBluescript. Individual clones were randomly sequenced and assigned according to their RNA derivation from the introduced cosmid *Xist* gene or from the endogenous CCE *Xist* gene.

DNA and RNA FISH. Metaphase spreads were obtained from ES cells and FISH was performed as described[8]. 100–200 ng biotinylated probe was used for hybridization, together with 2 μg mouse COT-1 DNA and 5 μg salmon sperm DNA. Slides were incubated overnight at 37 °C and washed stringently. Probe was detected using two rounds of FITC-conjugated avidin amplification. FISH signal detection was performed using a Zeiss Axioscop microscope equipped with epifluorescence and a triple-band-pass filter by analysis of digital images from a high-resolution CCD camera (Photometrics, USA) and imaging software (Digital Scientific). ES and differentiated cells were prepared for DNA/RNA FISH by modification of standard techniques[8]: ES cells were grown on gelatinized slides, fixed by air-drying, permeabilized with 0.5% Triton-X 100 in CSK (100 mM NaCl, 300 mM sucrose, 3 mM $MgCl_2$, 10 mM PIPES, pH 6.8) buffer and fixed with cold 4% paraformaldehyde. Slides were stored at 4 °C in 70% ethanol. Cell populations were enriched for differentiated cells by plating EBs grown without G418 selection in suspension for 4 days onto gelatinized dishes. The mixed population was then trypsinized and allowed to adhere to non-gelatinized tissue-culture dishes for 1 h, when non-adherent (ES) cells were aspirated and fresh medium added. This procedure was repeated following growth of plated cells for 2–3 days; however, cells were allowed to adhere to gelatinized glass slides. Slides containing differentiated cells were fixed and stored as described. Slides prepared for DNA/RNA FISH (Fig. 4) were dehydrated through an ethanol series to 100% ethanol, dried under vacuum, and hybridized overnight at 37 °C. Slides were washed and the biotin signal detected as described; as a control, some slides were treated with RNaseH before signal detection and fixation. The RNA signal was fixed for 5 min in 4% paraformaldehyde; slides were then dehydrated, denatured, dehydrated again and hybridized to a DIG-labelled DNA probe. The DNA signal was detected following a medium-stringency wash with Texas red-conjugated anti-sheep or rhodamine-conjugated anti-DIG antibodies. The *Xist* RNA probe was the biotin-labelled PCR product of *Xist* exons 1 and 6. X chromosome localization was achieved using a biotin- or biotin/DIG-labelled P1 clone (ICRFP703D1773; ref. 23) which maps to the telomeric region of the X chromosome (L.H., unpublished result).

Received 10 October 1996; accepted 31 January 1997.

1. Lyon, M. F. Gene action in the X chromosome of the mouse (*Mus musculus L.*). *Nature* **190,** 370–373 (1961).
2. Lyon, M. F. Some milestones in the history of X-chromosome inactivation. *Annu. Rev. Genet.* **26,** 16–28 (1992).
3. Rastan, S. X Chromosome inactivation and the *Xist* gene. *Curr. Opin. Genet. Dev.* **4,** 292–297 (1994).
4. Lee, J. T., Strauss, W. M., Dausman, J. A. & Jaenisch, R. A 450 kb transgene displays properties of the mammalian X-inactivation center. *Cell* **86,** 83–94 (1996).
5. Brown, C. J. *et al.* A gene from the region of the human X-inactivation centre is expressed exclusively from the inactive X chromosome. *Nature* **349,** 38–44 (1991).
6. Brockdorff, N. *et al.* Conservation of position and exclusive expression of mouse *Xist* from the inactive X chromosome. *Nature* **351,** 329–331 (1991).
7. Borsani, G. *et al.* Characterization of a murine gene expressed from the inactive X chromosome. *Nature* **351,** 325–329 (1991).
8. Clemson, C. M., McNeil, J. A., Willard, H. F. & Lawrence, J. B. *XIST* RNA paints the inactive X chromosome at interphase: evidence for a novel RNA involved in nuclear/chromosome structure. *J. Cell Biol.* **132,** 259–275 (1996).
9. Penny, G. D., Kay, G. F., Sheardown, S. A., Rastan, S. & Brockdorff, N. Requirement for *Xist* in X chromosome inactivation. *Nature* **379,** 131–137 (1996).
10. Rastan, S. & Robertson, E. J. X-chromosome deletions in embryo-derived (EK) cell lines associated with lack of X-chromosome inactivation. *J. Embryol. Exp. Morphol.* **90,** 379–388 (1985).
11. Rastan, S. Primary non-random X inactivation caused by controlling elements in the mouse demonstrated at the cellular level. *Genet. Res.* **40,** 139–147 (1982).
12. Herzing, L. & Ashworth, A. Construction of specific cosmids from YACs by homologous recombination in yeast. *Nucleic Acids Res.* **23,** 4005–4006 (1995).
13. Tan, S.-S., Williams, E. A. & Tam, P. P. L. X chromosome inactivation occurs at different times in different tissues of the post-implantation mouse embryo. *Nature Genet.* **3,** 170–174 (1993).
14. Matsuura, S., Episkopou, V., Hamvas, R. & Brown, S. Xist expression from an *Xist* YAC transgene carried on the mouse Y chromosome. *Hum. Molec. Genet.* **3,** 451–459 (1996).
15. Kay, G. F. *et al.* Expression of *Xist* during mouse development suggests a role in the initiation of X chromosome inactivation. *Cell* **72,** 171–182 (1993).
16. Palmiter, R. D. & Brinster, R. L. Germ-line transformation of mice. *Annu. Rev. Genet.* **20,** 465–499 (1986).
17. Hendrich, B. D., Brown, C. J. & Willard, H. F. Evolutionary conservation of possible functional domains of the human and murine *XIST* genes. *Hum. Molec. Genet.* **2,** 663–672 (1993).
18. Jeppesen, P. & Turner, B. M. The inactive X chromosome in female mammals is distinguished by a lack of histone H4 acetylation, a cytogenetic marker for gene expression. *Cell* **74,** 281–289 (1993).
19. RamirezSolis, R., Liu, P. & Bradley, A. Chromosome engineering in mice. *Nature* **378,** 720–724 (1995).
20. Gautier, C., Mehtali, M. & Lathe, R. A ubiquitous mammalian expression vector, pHMG, based on a housekeeping gene promoter. *Nucleic Acids Res.* **17,** 8389 (1989).
21. Friedrich, G. & Soriano, P. Promoter traps in embryonic stem cells: a genetic screen to identify and mutate developmental genes in mice. *Genes Dev.* **5,** 1513–1523 (1991).
22. Herzing, L. & Meyn, M. S. Novel *lacZ*-based recombination vectors for mammalian cells. *Gene* **137,** 163–169 (1993).
23. Lehrach, H. *et al.* in *Genome Analysis 1: Genetic and Physical Mapping* (eds Davies, K. E. & Tilghman, S. M.) 39–81 (Cold Spring Harbor Laboratory Press, Cold Spring Harbor, New York, 1990).

Supplementary Information is available on *Nature*'s World-Wide Web site (http://www.nature.com) or as paper copy from Mary Sheehan at the London editorial office of *Nature*.

Acknowledgements. We thank the Cancer Research Campaign for financial support. L.H. is the recipient of an NIH postdoctoral NRSA fellowship. We thank S. Duthie and C. Price for advice on FISH, and N. Brockdorff, M. Cullen, S. Palmer, D. Bertwistle and T. Enver for helpful comments on the manuscript.

Correspondence and requests for materials should be addressed to A.A. (e-mail: alana@icr.ac.uk).

Long-range *cis* effects of ectopic X-inactivation centres on a mouse autosome

Jeannie T. Lee*† & Rudolf Jaenisch*

* *Whitehead Institute for Biomedical Research, 9 Cambridge Centre, Cambridge, and Department of Biology, Massachusetts Institute of Technology, Massachusetts 02142, USA*

† *Pathology Department, Massachusetts General Hospital, 15 Fruit Street, Boston, Massachusetts 02114, USA*

In mammals, the X chromosome is unique in being capable of complete inactivation. Such X inactivation evolved to compensate for gene dosage differences between females with two X chromosomes and males with one[1]. Transcriptional silencing of a single female X chromosome is controlled *in cis* by *Xist*[2], whose RNA product coats the inactive X chromosome (X_i)[3], and the X-inactivation centre (*Xic*)[4]. A transgenic study limited the *Xic* to 450 kilobases including *Xist*, and demonstrated that it is sufficient

to initiate X inactivation[5]. Here we report that ectopic *Xist* RNA completely coats transgenic chromosome 12. Expression of genes over 50 centimorgans was reduced two-fold and was detected only from the normal homologue in fibroblasts. Moreover, ectopic *Xic* action resulted in chromosome-wide changes that are characteristic of the X_i: DNA replication was delayed, and histone H4 was markedly hypoacetylated. Our findings suggest long-range *cis* effects on the autosome similar to those of X inactivation, and imply that the *Xic* can both initiate X inactivation and drive heterochromatin formation. Thus, the potential for chromosome-wide gene regulation is not intrinsic to X-chromosome DNA, but can also occur on autosomes possessing the *Xic*.

X inactivation consists of several steps, including the counting of X chromosomes[2,6], commitment of all but one of these to inactivation[1], initiation at *Xic*[4,6], induction of *Xist* expression[7–9], propagation of *Xist* RNA along the X chromosome[3], and establishment and maintenance of heterochromatin throughout the X chromosome[10]. We had previously generated transgenic murine embryonic stem (ES) cell and fibroblast lines in which the *Xic* carried on the yeast artificial chromosome Y116 was transplanted onto autosomes in male cells[5]. We found that the 450-kb transgene recapitulated steps leading up to *Xist* expression and spread of *Xist* RNA into adjacent autosomal DNA. Here we investigated whether events initiated by ectopic *Xic*s can be completed on autosomes, and whether inactivation can occur independently of context or whether establishment and maintenance of heterochromatin require additional *cis*-acting elements specifically along the X chromosome.

To test whether the potential for large-scale inactivation lies in intrinsic differences between X and autosomal DNA, we examined *cis* effects of ectopic *Xic*s on the autosome in the male transgenic fibroblast line 116.6 (ref. 5). This line was isolated from mouse chimaeras derived from male ES cells carrying >20 tandem copies of Y116 in a 40XY background. However, because simian virus 40 (SV40) large T transformation was necessary for fibroblast cloning, each fibroblast line contains diploid (<30%) and tetraploid (>70%) cells. Like diploids, tetraploids inactivate all but one X chromosome per diploid genome. To identify the autosome of transgene insertion, we performed fluorescence *in situ* hybridization (FISH) using mouse chromosome-specific paints and the Y116 probe (Fig. 1a, b). Co-localization of Y116 signals and autosomal paints revealed a pericentromeric integration into chromosome 12 (Ch12).

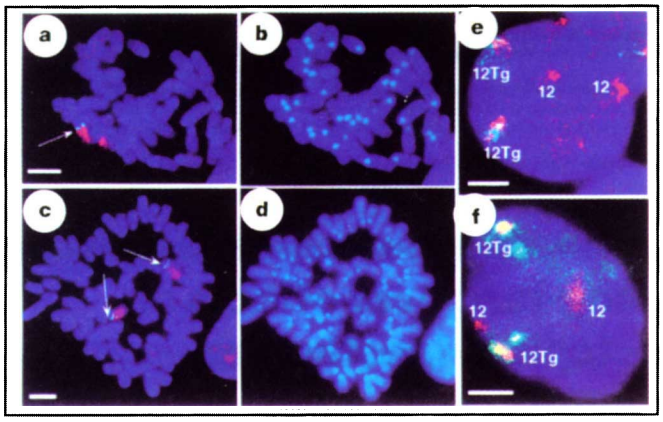

Figure 1 *Xist* RNA completely coats mouse Ch12. **a**, **b**, Mapping of transgene insertion site in ES line 116.6 by two-colour FISH (**a**) using FITC-labelled Y116 (green) and Texas red-labelled Ch12-specific paint (red), demonstrating pericentromeric insertion of the 20-copy transgene (arrow). The single-copy endogenous *Xic* is not evident because of short exposure time. Chromosomes were counterstained by DAPI (**b**). **c**, **d**, *Xist* RNA coats all of Ch12.Tg in metaphase ($n > 50$; note tetraploidy). To visualize *Xist* RNA, undenatured chromosomes were hybridized to rhodamine-labelled *Xist* probe. To detect Ch12.Tg, subsequently denatured chromosomes were probed with FITC-labelled Y116 (arrows). The two images are superimposed in **c**. Chromosomes were counterstained with DAPI (**d**). **e**, **f**, Localization of *Xist* RNA to the Ch12 domain in interphase nuclei ($n > 100$). Cytogenetically prepared cells (**e**) and cells grown *in situ* (**f**) were hybridized to FITC-labelled *Xist* probe, and subsequently denatured for hybridization to Texas-red conjugated Ch12-paint. Ch12.Tg (12Tg) and wild-type Ch12 (12) were distinguished in separate experiments by Y116 hybridization. Overlapping *Xist* and Ch12 signals are yellow-white. Scale bar, 5 μm.

To address whether *Xist* RNA can coat autosomes as it does the X_i, we examined interphase and metaphase chromosomes using two-colour FISH which simultaneously detected *Xist* RNA and Ch12. Over 95% of metaphases ($n > 50$) from the 116.6 fibroblasts demonstrated spread of *Xist* RNA throughout transgenic Ch12 (Ch12.Tg; Fig. 1c, d). Apart from the centromere, there were no apparent skip regions. The RNA did not bind other chromosomes, including the X. Association was also observed during interphase when *Xist* RNA localized to the Ch12 domain in cells prepared using two fixation techniques (Fig. 1e, f). Thus *Xist* RNA can associate with the autosome as it does with the X_i, and exhibits the same *cis*-restriction at the ectopic locus. In contrast to human *XIST* RNA[3], murine *Xist* associates stably with both X_i (B. Panning, unpublished data) and Ch12 during interphase and mitosis until late metaphase.

The genetic distance of Ch12 is 60–70 cM (ref. 11). To examine effects on transcription, we assayed expression of Ch12-linked housekeeping genes at various distances (Fig. 2a)[11]: *Rrm2* (ribonucleotide reductase M2) at 7 cM from the centromere, *mSos2* at 30 cM, c-*Fos* at 40 cM, and *Yy1* at 53 cM. We used quantitative reverse transcription–polymerase chain reaction (RT–PCR)[12] to investigate whether Ch12 gene expression is reduced in transgenic fibroblasts compared with control isogenic fibroblasts. Quantitization was made possible by amplifying in the exponential phase and normalizing to expression of *Dnmt*, a housekeeping gene on Ch9. Expression of *Rrm2* and *mSos2* was twofold lower in transgenic ($n = 8$) than in control mice ($n = 8$) (Mann-Whitney test, $P < 0.001$; Fig. 2b, c, e). Importantly, these differences did not result from aneuploidies, as Ch9 and Ch12 were present at two copies per diploid genome (four in tetraploids) in transgenic and control mice, as demonstrated by chromosome painting (data not shown). In contrast, there was no reduction ($P > 0.13$; Fig. 2d, e) for the unlinked gene ribosomal protein L7 (*RpL7*) residing on Ch2 (also not aneuploid).

We used RNA FISH to visualize nascent *Yy1* and c-*Fos* expression. As c-*Fos* is induced by serum, control and transgenic fibroblasts were grown for 24 h in serum-free DME, then induced by 20% fetal bovine serum/DME, and paraformaldehyde-fixed after 15 min (ref. 13). RNA FISH was performed without DNA denaturation to exclude DNA detection. The authenticity of RNA signals was established by subsequent hybridization to Ch12 paint or to the subtelomeric marker D12mit196 (data not shown). In control female cells, c-*Fos* RNA was visible in 40% of serum-induced cells and in 5% of uninduced cells, consistent with previous observation[13]. *Yy1* RNA could be seen in 30% of cells regardless of whether induction had occurred. To determine the origin of c-*Fos* and *Yy1* transcription in 116.6 fibroblasts, nascent RNA signals were scored for co-localization to *Xist* RNA, which marks the Ch12.Tg domain. Three patterns of expression were found (Fig. 3): (1) nascent RNAs not overlapping with *Xist* RNA (scored as monoallelic from wild-type Ch12); (2) nascent RNAs originating from within *Xist* RNA domains and from external loci (scored as biallelic); and (3) no detectable nascent RNA. In tetraploids, a signal from one or both copies of Ch12 or Ch12.Tg was scored as expression. In controls expressing c-*Fos*, the predominant pattern was biallelic (67 of 70); in transgenic cells, the predominant pattern was monoallelic (57 of 61; Fig. 3a, c). Similarly, *Yy1* was predominantly biallelic in controls (33 of 40) but mostly monoallelic

in transgenics (48 of 69). However, a significant portion of transgenic cells expressing *Yy1* did so from Ch12.Tg (21 of 69; Fig. 3b, c). This implies that there was escape from *Yy1* inactivation in some cells.

The results of quantitative RT–PCR and RNA FISH indicate downregulation of genes *in cis* to the transgene suggestive of transcriptional inactivation. This is consistent with our previous finding that *lacZ*, a marker carried on the Y116 vector, was silenced in 116.6 fibroblasts[5]. If silencing mediated by ectopic *Xic*s resembled X inactivation, the transgenic autosome may acquire biochemical changes found on the X_i. Delayed replication timing is strongly correlated with gene silencing in yeast, *Drosophila* and mammals, in which the two events are controlled by the same elements[14]. The X_i replicates later in S phase than euchromatin and replicates asynchronously with its active homologue[15]. We tested whether the transgene altered Ch12.Tg replication by incorporation of bromodeoxyuridine (BrdU) during DNA synthesis. To identify the late S-phase window, we pulse-labelled non-synchronized control cultures with BrdU for 30 min at various time intervals before the cells were collected. Cells pulsed at −7 h labelled autosomes and the active X, whereas cells pulsed at −4 to −6 h show labelling of the X_i and Y, thus establishing that late S occurs at −4 to −6 h.

In 32 transgenic metaphases examined from three independent lines during this S-phase window, two distinct chromosomes were labelled (Fig. 4). Ch12 and Y116 hybridization indicated that Ch12.Tg was uniquely labelled in 25 of 32 spreads. In three metaphases, the Y (identified by DAPI appearance) was solely labelled. In the remaining four spreads, both Ch12.Tg and the Y incorporated BrdU. Because the Y also replicates late in S[16], co-labelling of the Y and Ch12.Tg independently confirmed delayed replication for Ch12.Tg (however, because a 30-min pulse identified only a narrow window in S phase (5 h), Y and Ch12.Tg did not always label together). No other chromosome, including wild-type Ch12, demonstrated delayed BrdU incorporation. These results indicate that, like the X_i, Ch12.Tg replicates late and asynchronously with its homologue.

A direct relationship between histone acetylation and transcription has been demonstrated, as acetylation of histone H4 correlates strongly with gene activity[17,18]. In mammals, the female X_i is hypoacetylated at all four amino-terminal lysines[19]. To determine whether H4-deacetylation occurs on Ch12.Tg, metaphase chromosomes from 116.6 ES cells and fibroblasts were immunostained with antibodies R17 (which binds all four acetylated isoforms) and R41/5 (which binds lys-5-acetylated isoform)[19]. In undifferentiated transgenic ES cells, no chromosome was detectably hypoacetylated (Fig. 5); in contrast, two chromosomes were hypoacetylated in 90% of tetraploid fibroblast nuclei (Fig. 5a, b, e). When five independently cloned lines were examined, Ch12 painting and Y116 probes revealed that the underacetylated chromosome was invariably Ch12.Tg, and that the wild-type homologue achieved acetylation

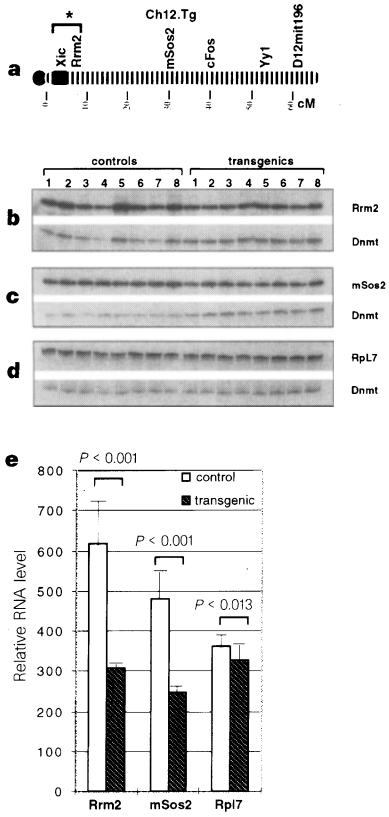

Figure 2 Gene expression from Ch12 is reduced twofold. **a**, Genetic map of Ch12 indicating approximate locations of housekeeping genes and microsatellite markers used in this study. Asterisk indicates that the relative positions of *Rrm2* and the transgene have not been established. **b**–**d**, Quantitative RT-PCR of *mSos2*, *Rrm2* and *RpL7* (Ch2), coamplified with *Dnmt* (Ch9). Eight clones of fibroblast 116.6 and control isogenic fibroblast lines were used for analysis, none of which were aneuploid for Ch2, 9 and 12. PCR was performed in the exponential phase and all product levels were standardized to *Dnmt*. To ensure that only cDNA and not genomic DNA was amplified, RT-PCR was performed on +RT and −RT samples; −RT controls did not amplify (data not shown). **c**, Summary of relative gene expression. Averages and standard deviations were as follows, given as mean (s.d.): *Rrm2*, control 618, (110), Tg 306 (9). *mSos2*, control 481 (84), Tg 247 (17). *RpL7*, control 361 (29), Tg 326 (46). The Mann–Whitney rank-sum test was used to determine statistical significance of the differences (*P*-values shown above each pair).

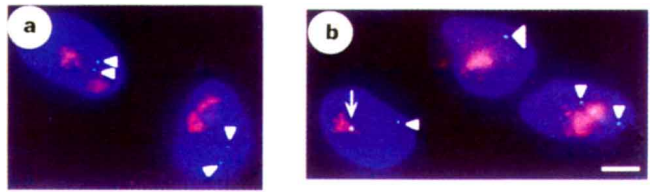

c

	c-Fos		Yy1	
	Control (n = 167)	Transgenic (n = 182)	Control (n=143)	Transgenic (n= 230)
monoallelic				
Ch12	3 (2%)	57 (32%)	7 (5%)	48 (21%)
Ch12.Tg	-	0 (0%)	-	9 (4%)
biallelic	67 (40%)	4 (2%)	33 (23%)	12 (5%)
no expression	97 (58%)	121 (66%)	103 (72%)	161 (70%)

Figure 3 c-*Fos* and *Yy1* are monoallelically expressed in 116.6 fibroblasts. **a**, **b**, Serum-induced 116.6 fibroblasts hybridized to Texas-red-labelled *Xist* and FITC-labelled c-*Fos* (**a**) or *Yy1* (**b**). To visualize c-*Fos* and *Yy1* nascent transcript, a 4.4-kb murine c-*Fos* genomic probe (p302-356 pBS(−))[13] and 1.8-kb murine *Yy1* cDNA probe (pδ)[30] were used. Double photographic exposures were taken to determine the relative positions of nascent transcripts to *Xist* RNA. Ploidy was inferred from number of *Xist* signals; the reliability of the method was determined in separate experiments which established that diploids have one *Xist* signal and tetraploids have two **a**, Arrowheads indicate c-*Fos* transcription from wild-type Ch12 (cells are tetraploid). **b**, Arrowheads indicate *Yy1* transcription from wild-type Ch12; the arrow indicates expression from Ch12.Tg (note both diploid and tetraploid nuclei in this field). Scale bar, 5 μm. **c**, Distribution of monoallelic and biallelic expressers for c-*Fos* and *Yy1* in controls and transgenics; *n* is the sample size.

equal to that of other autosomes. In a minority (~10%) of some clonal cultures, the transgenic autosome was hypoacetylated on only the proximal half (Fig. 5c–e), which suggests that there must be some instability in the maintenance of chromatin structure. This is consistent with our finding that *Yy1* escapes inactivation in some cells (Fig. 3c). Although the Y was late replicating, it was not consistently underacetylated (2 out of 49; Fig. 5c, d). These data indicate that differentiation resulted in autosomal hypoacetylation similar to that of the X_i.

Our results therefore suggest that the *Xic* transgene affects chromatin structure and gene expression over a distance of 50 cM of the autosome. The ectopic loci enable Ch12 to exist either as an early-replicating, acetylated and presumably active chromosome, or as a late-replicating, hypoacetylated and probably inactive chromosome. These results imply that the *Xic* not only initiates X inactivation[5] but also drives long-range heterochromatin formation. Furthermore, neither binding to *Xist* RNA nor the potential for chromosome-wide gene regulation is intrinsic to the X. Thus inactivation in our transgenic system does not absolutely require X-specific elements in propagation and/or stabilization of heterochromatin, and indicates that an *Xic in cis* is the primary requirement for the inactivation process. This contrasts with dosage compensation in *Drosophila*, which depends on such X-specific elements; autosome segments inserted into the male X are not dosage compensated, and X-linked genes inserted into autosomes remain partly compensated[20]. However, this is consistent with mouse transgenic experiments, in which autosomal genes inserted into the X became subject to inactivation[21] and, conversely, where X-linked genes inserted into autosomes were not dosage compensated[22]. Overt differences with human and mouse X-autosome translocations where spread of autosomal inactivation is variable and limited[23,24] could reflect *in vivo* selection against cells in which complete autosomal inactivation led to haplo-insufficiency.

Our results demonstrate that long-range *cis* effects occur on autosomal DNA, but further work is required to determine whether silencing includes all autosomal genes. Furthermore, as some genes on the X_i are only partly inactivated[25,26], it is not yet clear whether *Xic*-mediated inactivation results in complete transcriptional repression of affected genes. *Xic*-mediated effects on autosomes may be less stable than on the X chromosome. Indeed, our study suggests that there is instability of either propagation or maintenance of heterochromatin on Ch12, as demonstrated by reacetylation of distal Ch12.Tg and sporadic escape of *Yy1* expression. Our unpublished results on other Y116 transgenics containing ~6 copies integrated into Ch10 (116.7)[5] or 2–3 copies subtelomerically on Ch11 (116.13)[5] suggest there are further complexities in the silencing mechanism. As differentiating ES cells, *Xist* RNA was expressed abundantly and showed *cis*-association with Ch10 and Ch11. However, expression and associated *cis*-effects were selected against in fibroblasts isolated from chimaeric mice (so this study could only be performed on 116.6). Varying sites of integration, *Xic*

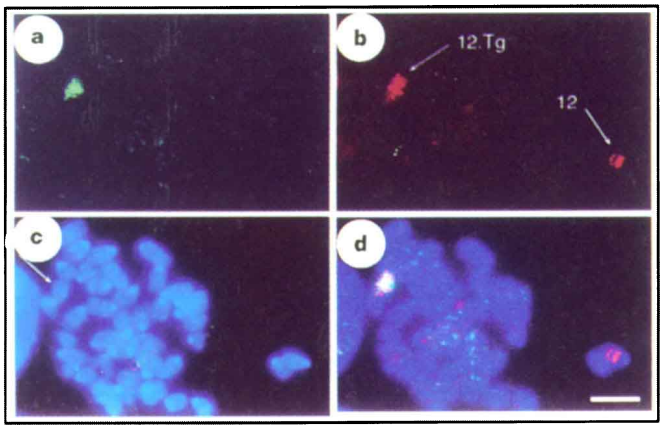

e

BrdU-labelled chromosomes per metaphase	*n*
Ch12.Tg only	25
Y only	3
Ch12.Tg + Y	4
Other chromosomes	0

Figure 4 Ch12.Tg replicates late in S phase and asynchronously with its homologue. The 116.6 fibroblasts were pulse-labelled with BrdU for 30 min in the late S-phase window. **a**, Indirect immunofluorescence with anti-BrdU antibodies (Sigma) to detect BrdU-labelled chromosomes. **b**, FISH analysis with Ch12-paint detected by avidin-Texas red. Wild-type Ch12 (12) and Ch12.Tg (12.Tg) were distinguished by hybridization to Y116 (not shown). **c**, DAPI-counterstained chromosomes. Arrow, Ch12.Tg. **d**, Merging of **a**–**c**. **e**, The frequency with which Ch12.Tg and the Y were BrdU-labelled during late S phase. Scale bar, 5 μm.

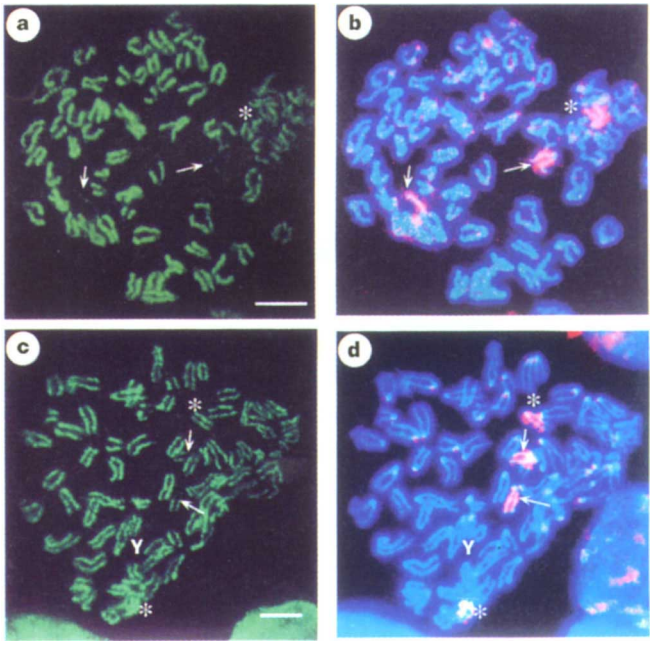

e

Ch12.Tg acetylation pattern	ES cells	Fibroblasts
Tg	26	0
	0	45
	0	4

Figure 5 Histone H4 is hypoacetylated on Ch12.Tg. Metaphase chromosomes from 116.6 fibroblasts were immunolabelled with R17 (recognizing all acetylated H4 isoforms) or R41/5 (specific for acetylated lys-5 isoform)[19] and indirectly detected by FITC. As results were similar with both antibodies, data are shown for only R17. **a**, Tetraploid metaphase chromosomes showing two hypoacetylated chromosomes (arrows), revealed in separate experiments to be Ch12.Tg by Y116 FISH (not shown). **b**, Same metaphase counterstained with DAPI and hybridized to Ch12 paint. Arrows, underacetylated Ch12.Tg; asterisks, fully acetylated wild-type Ch12. The second wild-type Ch12 is outside the field shown. **c**, In a minority of cells from some clones, Ch12.Tg is hypoacetylated only on the proximal half (arrows). Note the Y is also underacetylated. **d**, DAPI staining and Ch12 painting of the metaphase in **c**. **e**, Acetylation patterns and frequencies in 116.6 ES cells and fibroblasts. Stippled regions, acetylated. Scale bar, 5μm.

copy number, and choice of cell types could all explain the observed differences. Future work is required to address whether *cis* effects result from *Xist* action alone or require additional function from the *Xic*.

Methods

Quantitative RT-PCR. Total cellular RNAs from mitotically active transgenic and control fibroblasts were prepared using RNAzol B (TelTest) as recommended. After DNaseI digestion, first-strand cDNA was synthesized from 2 μg of RNA[5]. For RT–PCR, 0.25 μg of cDNA was amplified with 5 U Taq polymerase (Promega), 1.5 mM $MgCl_2$, 200 μM dNTPs, and 250 nM each of *Dnmt* primers, *Sal5′* and *Sal3′*B[5] and primers for *RpL7*, *Rrm2* and *mSos2* as follows: RpL7A, 5′-GAAGCTCATCTATGAGAAGGC-3′; RpL7B, 5′-AAGACGAAGGAGCTGCAGAAC-3′; Rrm2A, 5′-AAGCGACTCACCCTGGCTGAC-3′; Rrm2C, 5′-GACTATGCCATCACTCGCTGC-3′; Sos2B, 5′-CTGGCCATGATTGGGTTTACA-3′; Sos2C, 5′-TATGTCCTTCCACGCCTCATG-3′. DNAs were denatured at 95 °C, 45 s; annealed at 55 °C, 45 s; and extended at 72 °C, 90 s. For quantification, primers *Sal3′*B, Rrm2C, Sos2C, and RpL7B were phosphorylated with polynucleotide kinase and [γ-^{32}P]ATP. PCR products were analysed in 6% polyacrylamide/8 M urea gels and quantified by phosphorimaging (Fujix BAS2000 BioImaging Analyzer and MacBas v2.2). Standard PCR curves for all genes were generated, indicating exponential amplification between 10 and 23 cycles; 20 cycles was chosen for all reactions. For the standard curve, a master mix of reagents was apportioned equally among 16 reaction tubes; PCR of 0.25 μg of control female cDNA was sampled every two cycles from 10–40 cycles.

FISH. Interphase nuclei and chromosome spreads for FISH were prepared by cytogenetic[27] or *in situ*[28] techniques. Probes were prepared by random priming with digoxigenin-11-dUTP or biotin-16-dUTP (Boehringer) and detected with anti-digoxigenin:rhodamine (Sigma) or avidin:FITC (Vector). Mouse chromosome-specific painting was performed as recommended (Applied Genetics Laboratory). *Xist* RNA was detected by λ13.7 probe encompassing exon 1 and the promoter, and controls for ensuring detection of RNA, not DNA, were performed[5].

DNA replication timing. Cultures were pulse-labelled with BrdU for 30 min, treated with 10 μg ml^{-1} colchicine for 2 h before collection, 3–8 h after labelling. Detection of BrdU was performed[29] on metaphase chromosomes prepared by standard technique[27]. Spreads containing late-replicating chromosomes were photographed with the Zeiss Axioskip/MC80 camera on 1600 Ektachrome film. Their stage coordinates were noted for overlaying with FISH results. To identify late-replicating chromosomes, slides were washed 3 times in 4 × SSC/0.1% Tween 20 for 5 min, at 45 °C, denatured in 70 mM NaOH + 70% ethanol for 3 min dehydrated in 80% and 100% ethanol for 2 min each, and subjected to FISH using Y116 and Ch12 painting probes. FISH results were photographed and overlaid with BrdU images in Photoshop 3.0.

Histone H4 acetylation. Chromosomes for immunostaining were prepared[20], photographed and marked by stage coordinates. To identify hypoacetylated chromosomes, slides were washed 3 times in 4 × SSC/0.1% Tween 20, then denatured in 2 × SSC/70% formamide at 72 °C for 5 min, and standard FISH results were photographed and overlaid with hypoacetylated chromosomes in Photoshop 3.0.

Received 30 October 1996; accepted 24 January 1997.

1. Lyon, M. F. Gene action in the X-chromosome of the mouse (*Mus musculus* L.). *Nature* **190,** 372–373 (1961).
2. Penny, G. D., Kay, G. F., Sheardown, S. A., Rastan, S. & Brockdorff, N. Requirement for *Xist* in X chromosome inactivation. *Nature* **379,** 131–137 (1996).
3. Clemson, C. M., McNeil, J. A., Willard, H. & Lawrence, J. B. XIST RNA paints the inactive X chromosome at interphase: evidence for a novel NA involved in nuclear/chromosome structure. *J. Cell Biol.* **132,** 1–17 (1996).
4. Rastan, S. & Brown, S. D. M. The search for the mouse X-chromosome inactivation centre. *Genet. Res.* **56,** 99–106 (1990).
5. Lee, J. T., Strauss, W. M., Dausman, J. A. & Jaenisch, R. A 450 kb transgene displays properties of the mammalian X-inactivation center. *Cell* **86,** 83–94 (1996).
6. Rastan, S. J. Non-random X-chromosome in mouse X-autosome translocation embryos–location of the inactivation centre. *Embryol. Exp. Morphol.* **78,** 1–22 (1983).
7. Brown, C. J. *et al.* The human XIST gene: analysis of a 17 kb inactive X-specific RNA that contains conserved repeats and is highly localized within the nucleus. *Cell* **71,** 527–542 (1992).
8. Brockdorff, N. *et al.* The product of the mouse Xist gene is a 15 kb inactive X-specific transcript containing no conserved ORF and located in the nucleus. *Cell* **71,** 515–526 (1992).
9. Kay, G. F. *et al.* Expression of Xist during mouse development suggests a role in the initiation of X chromosome inactivation. *Cell* **72,** 161–182 (1993).
10. Brown, C. J. & Willard, H. F. The human X-inactivation centre is not required for maintenance of X-chromosome inactivation. *Nature* **368,** 154–156 (1994).
11. D'Eustachio, P. Mouse chromosome 12. *Mamm. Genome* **5,** S181–S195 (1994).
12. Foley, P. F., Leonard, M. W. & Engel, J. D. Quantitation of RNA using the polymerase chain reaction. *Trends Genet.* **9,** 380–385 (1993).
13. Huang, S. & Spector, D. L. Nascent pre-mRNA transcripts are associated with nuclear regions enriched in splicing factors. *Genes Dev.* **5,** 2288–2302 (1991).
14. Bell, S. P., Kobayashi, R. & Stillman, B. Yeast origin recognition complex functions in transcription silencing and DNA replication. *Science* **262,** 1844–1849 (1993).
15. Priest, J. H., Heady, J. E. & Priest, R. E. Delayed onset of replication of human X chromosomes. *J. Cell Biol.* **35,** 483–487 (1967).
16. Schempp, W. in *The Y Chomosome* (ed. Sandberg, A. A.) 357–371 (Alan R. Liss, New York, 1985).
17. Wolffe, A. P. & Pruss, D. Targeting chromatin disruption: transcription regulators that acetylate histones. *Cell* **84,** 817–819 (1996).
18. Turner, B. M., Birley, A. J. & Lavender, J. Histone H4 isoforms acetylated at specific lysine residues define individual chromosomes and chromatin domains in *Drosophila* polytene nuclei. *Cell* **69,** 375–384 (1992).
19. Jeppesen, P. & Turner, B. M. The inactive X chromosome in female mammals is distinguished by a lack of histone H4 acetylation, a cyrogenetic marker for gene expression. *Cell* **74,** 281–289 (1993).
20. Lucchesi, J. C. & Manning, J. E. Gene dosage compensation in *Drosophila melanogaster. Adv. Genet.* **24,** 371–429 (1987).
21. Krumlauf, R., Chapman, V. M., Hammer, R. E., Brinster, R. & Tilghman, S. M. Differential expression of α-fetoprotein genes on the inactive X chromosome in extraembryonic and somatic tissues of a transgenic mouse line. *Nature* **319,** 224–226 (1986).
22. Pravtcheva, D. D., Adra, C. N. & Ruddle, F. H. The timing of paternal Pgk-1 expresison in embryos of transgenic mice. *Development* **111,** 1109–1120 (1991).
23. Keitges, E. A. & Palmer, C. G. Analysis of spreading of inactivation in eight X autosome translocations utilizing the high resolution RBG technique. *Hum. Genet.* **72,** 230–236 (1986).
24. Eicher, E. M. X-autosome translocations in the mouse: total inactivation versus partial inactivation of the X chromosome. *Adv. Genet.* **15,** 175–259 (1970).
25. Carrel, L., Hunt, P. A. & Willard, H. F. Tissue and lineage-specific variation in inactive X chromosome expression of the murine Smcx gene. *Hum. Mol. Genet.* **5,** 1361–1366 (1996).
26. Sheardown, S., Norris, D., Fisher, A. & Brockdorff, N. The mouse Smcx gene exhibits developmental and tissue specific variation in degree of escape from X inactivation. *Hum. Mol. Genet.* **5,** 1355–1360.
27. Trask, B. J. Fluorescence in situ hybridization. *Trends Genet.* **7,** 149–154 (1991).
28. Lawrence, J. B., Singer, R. H. & Marselle, L. M. Highly localized tracks of specific transcripts within interphase nuclei visualized by in situ hybridization. *Cell* **57,** 493–502 (1989).
29. Vogel, W., Autenrieth, M. & Speit, G. Detection of bromodeoxyuridine-incorporation in mammalian chromosomes by a bromodeoxyuridine-antibody. *Hum. Genet.* **72,** 129–132 (1986).
30. Hariharan, N., Kelley, D. E. & Perry, R. P. d, a transcription factor that binds to downstream elements in several polymerase II promoters, is a functionally versatile zinc finger protein. *Proc. Natl Acad. Sci. USA* **88,** 9799–9803 (1991).

Acknowledgements. We thank J. Dausman for maintaining the mouse colony; B. Turner, and A. Keohane for providing antibodies and protocols for detecting acetylated H4; S. Huang for p302-356pBS(−) and Y. Shi for pδ; C. Beard and B. Panning for discussion; and J. Kirby, R. Chen, Y.-K. Wang and Y. Marahrens for critical reading of the manuscript. This work was funded by a Howard Hughes Medical Institute fellowship for physicians to J.T.L. and an NIH grant to R.J.

Correspondence and requests for materials should be addressed to J.T.L. (e-mail: jlee@wi.mit.edu) or R.J. (e-mail: jaenisch@wi.mit.edu).

GRIP: a synaptic PDZ domain-containing protein that interacts with AMPA receptors

Hualing Dong*†, Richard J. O'Brien*†‡, Eric T. Fung*†, Anthony A. Lanahan†, Paul F. Worley† & Richard L. Huganir†*

* *Howard Hughes Medical Institute,* † *Department of Neuroscience,*
‡ *Department of Neurology, Johns Hopkins University School of Medicine, Baltimore, Maryland 21205, USA*

AMPA glutamate receptors mediate the majority of rapid excitatory synaptic transmission in the central nervous system[1,2] and play a role in the synaptic plasticity underlying learning and memory[3,4]. AMPA receptors are heteromeric complexes of four homologous subunits (GluR1–4) that differentially combine to form a variety of AMPA receptor subtypes[1,2]. These subunits are thought to have a large extracellular amino-terminal domain, three transmembrane domains and an intracellular carboxy-terminal domain[5]. AMPA receptors are localized at excitatory synapses and are not found on adjacent inhibitory synapses enriched in $GABA_A$ receptors[6]. The targeting of neurotransmitter receptors, such as AMPA receptors, and ion channels to synapses is essential for efficient transmission[7,8]. A protein motif called a PDZ domain is important in the targeting of a variety of membrane proteins to cell–cell junctions including synapses[8–10]. Here